ARTICLES

Spectroscopy and Photophysics of Self-Organized Zinc Porphyrin Nanolayers. 1. Optical Spectroscopy of Excitonic Interactions Involving the Soret Band

Harry Donker,* Rob B. M. Koehorst, and Tjeerd J. Schaafsma

Laboratory for Biophysics, Department of Agrotechnology and Food Sciences, Wageningen University, Dreijenlaan 3, 6703 HA Wageningen, The Netherlands

Received: February 16, 2005; In Final Form: May 19, 2005

The photophysical properties of excited singlet states of zinc tetra-(*p*-octylphenyl)-porphyrin in 5−25-nm-thick films spin-coated onto quartz slides have been investigated by optical spectroscopy. Analysis of the polarized absorption spectra using a dipole−dipole exciton model with two mutually perpendicular transition dipole moments per molecule shows that the films are built from linear aggregates, i.e., stacks with a slipped-deck-of-cards configuration. The molecular planes of the porphyrins in the stacks are found to be perpendicularly oriented with respect to the substrate plane. Assuming a value of 2−3 for the dielectric constant of the film, from the excitonic shift, an angle of 44° ± 3° and an interplanar distance of 0.35−0.36 nm between adjacent porphyrins are calculated, close to the ground-state geometry in solution. The ordering in these films was further investigated by the effects of various solvents and temperature annealing. Spin-coating from toluene as a solvent results in highly ordered films, and annealing of these films has little effect on their absorption spectra. However, spin-coating from chloroform or pyridine or exposure of the films to these solvents in their vapor phases changes their ordering presumably due to incorporation of residual solvent molecules. Annealing yields absorption spectra identical to those of films spin-coated from toluene. The absorption spectra are insensitive to atmospheric moisture, in contrast to those of zinc tetraphenylporphyrin films lacking octyl substituents.

Introduction

This paper on excitonic interactions in the second excited singlet state of zinc tetra-(*p*-octylphenyl)-porphyrin (ZnTOPP) (Figure 1) is the first of a series of three closely related papers reporting the spectroscopic and photophysical properties of the first and second excited singlet states as well as the lowest excited triplet state in 5−25-nm-thick, self-organized films of this porphyrin on quartz slides as a substrate and the effects of various solvents and temperature annealing on their degree of order. The following paper treats excitation transport in these films studied by doping with varying concentrations of fluorescence quenchers. Finally, the results of magnetic resonance spectroscopy of triplet states in the porphyrin films are reported and discussed in the third paper.

There is a rapidly growing interest in the properties of organic films with nanometer thicknesses in optoelectronic devices as a result of the relatively simple deposition methods, low processing costs, and a large variety of molecular structures as compared to those of inorganic layers. During the past decade, the number of applications of inorganic films has rapidly increased,[1,2] and a breakthrough of nanoscale organic film technology appears to be just around the corner.[3,4] These kinds of films have a broad spectrum of potential applications, ranging from photo detectors, light-emitting diodes, sensors, solar cells, data storage devices, and displays to coatings for (bio)molecular recognition or nonlinear optics. For almost all of these applications, the creation, recombination, and transport of excitons and/or charge carriers play an essential role. A drawback of organic films is their usually low conductivity and dielectric constant, so that charge separation is energetically less favorable.[5] This drawback may be partially compensated by the ordering of these materials at the molecular scale, increasing the efficiency of these transport processes. Several recent reviews cover the progress of research on organic films.[6−8]

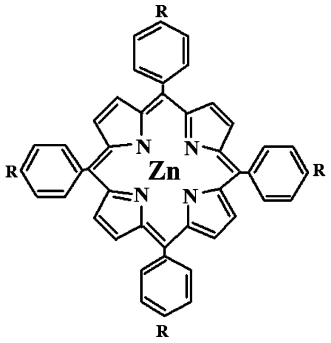

Figure 1. Molecular structure of zinc tetra-(*p*-octylphenyl)-porphyrin; R = $-C_8H_{17}$.

The optoelectronic properties of the films are largely determined by the degree of molecular ordering, the domain size,

* Author to whom correspondence should be addressed. Present address: Laboratory for Inorganic Chemistry, Delft University of Technology, Delft, The Netherlands. Phone: +31-15-2783891. Fax: +31-15-2788047. E-mail: H.Donker@tnw.tudelft.nl.

10.1021/jp058054o CCC: $30.25
Published on Web 08/18/2005

the distance and orientation of the molecules with respect to each other and to the substrate, and the optical, electric, and electrochemical properties of the film as well as those of the substrate.[9] In particular, tetrapyrrole compounds, such as porphyrins and phthalocyanines, and their supramolecular assemblies[10] offer fascinating options due to their self-organizing and steric properties,[11−17] stability, optical absorption in the visible range, and variability. The electrochemical properties can be controlled by varying the metal center, whereas the molecular architecture of the films is determined by substituting suitable functionalizing side groups.[18]

The orientation of the porphyrins with respect to the substrate in nanolayers is essential for most applications, which require anisotropic transport of excitons or charge carriers to the substrate. Much progress has been made in controlling and changing the orientation of porphyrins in such systems.[19−22]

Experimental Section

Thin ZnTOPP films of up to several tenths of nanometers in thickness on quartz plates (Suprasil, ∅ 15 mm, 1-mm-thickness) were prepared by spin-coating at 2500 rpm from 1−5 mM toluene, pyridine, or chloroform solutions. Before spin-coating, the quartz plates were subsequently rinsed with aqua regia, water, methanol, and toluene and blown dry with nitrogen. Through the use of the optical density of the films at 550 nm, their estimated thicknesses were 5−25 ± 5 nm, respectively. For the thickest film (25 nm), the amount of deposited porphyrin was also determined by dissolving the film in a known volume of toluene. Through the use of the extinction coefficient,[23] $\epsilon_{550} = 22\,000$ L M cm^{-1}, the calculated thickness was in good agreement with the above-mentioned value and corresponded to ∼100 porphyrin layers for the investigated film. All solvents were p.a. quality, unless stated otherwise. Films of the analogous compounds without alkyl chains, i.e., tetraphenyl porphyrins (TPP), were used as references.

ZnTOPP and ZnTPP were prepared by metallization of H_2-TOPP and H_2TPP, respectively, by refluxing in dimethylformamide (DMF) with $ZnCl_2$ (Merck, p.a.).[24] H_2TOPP and H_2TPP were synthesized by condensation of 4-(*n*-octyl)benzaldehyde and benzaldehyde (Kodak, 99%), respectively, with pyrrole (Janssen Chimica, 99%) in refluxing propionic acid (Merck, z.s.).[25,26] The porphyrins were purified by chromatography on silica (Merck, silica gel 60) with toluene or chloroform as the eluent. For duplicate samples, ZnTOPP purchased from Porphyrin Products was used. All porphyrins are estimated to be >99% pure as shown by thin-layer chromatography, absorption, and fluorescence spectroscopy.

Throughout this paper, films spin-coated from toluene are named films **1**, those spin-coated from chloroform films **2**, those spin-coated from toluene and subsequently exposed to chloroform vapor films **3**, and those spin-coated from pyridine films **4**.

Absorption spectra of spin-coated films were recorded on a Cary 5E spectrophotometer, equipped with an integrating diffuse reflectance sphere (DRA-CA-50, Labsphere), varying the angle between the normal of the substrate and the incident light beam between 10° and 50° The absorption spectra are uncorrected for reflection since the films are highly anisotropic, as is evident from the absorption spectra. Polarized absorption spectra were recorded by placing sheet polarizers (Polaroid type HNP′B) in the sample and reference beams, with their polarization direction either perpendicular (A_s) or parallel (A_p) to the plane of incidence of the incoming light.

Fluorescence spectra were recorded at room temperature using a Spex Fluorolog 3-22 fluorometer equipped with a 450-W xenon lamp as an excitation source. Spectra were measured in the front-face mode at an angle close to 0° or in the right-angle mode at ∼45° between the normal to the substrate and the incident light beam. Excitation spectra were corrected for lamp output, and emission spectra were corrected for photomultiplier sensitivity. Both types of spectra were also corrected for the monochromator transmission. Low-temperature (1.4 K) fluorescence measurements were carried out using a homemade liquid helium bath cryostat and a CW Ar^+ ion laser (Coherent CR-5) as excitation source. Emission light was selected with an OG 540 cutoff filter and a Jobin-Yvon HR1000 monochromator and detected with an S20 (EMI) photomultiplier.

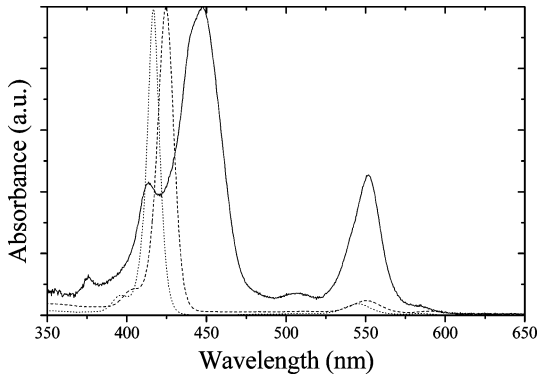

Figure 2. Absorption spectra of ZnTOPP in toluene (dashed line), hexane (dotted line), and a film spin-coated from 5 mM toluene solution onto quartz (solid line). The absorption spectrum of the spin-coated film was obtained with unpolarized light at an incidence angle of 10° and is uncorrected for reflection effects. For clarity, the spectra have been scaled to the same height.

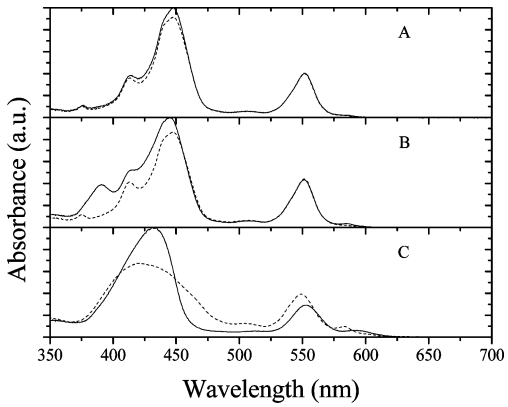

Figure 3. Absorption spectra of (A) a ZnTOPP film spin-coated from 5 mM toluene solution, (B) a ZnTOPP film spin-coated from 5 mM chloroform solution, and (C) a ZnTPP film spin-coated from 5 mM chloroform solution. Solid lines are before, dashed lines after 5 min of annealing at 175 °C. The spectra have been scaled to the highest intensity in the unannealed films.

Results and Discussion

Absorption Spectra. Absorption spectra of spin-coated ZnTOPP and ZnTPP films and solutions in toluene and hexane are shown in Figures 2 and 3. The spectra of the films are uncorrected for reflection effects. Results for purchased and home-synthesized ZnTOPP were identical.

The absorption spectra of ZnTOPP and ZnTPP are similar to those of a number of other porphyrins.[23] The weak bands at ∼585 (film), 590 (toluene), and 584 nm (hexane) are assigned to the Q(0,0) transition, the bands at ∼550 (film, toluene) and 546 nm (hexane) to the Q(1,0) transition, and the weak band at 507 (film), 515 (toluene), and 509 nm (hexane) to the Q(2,0)

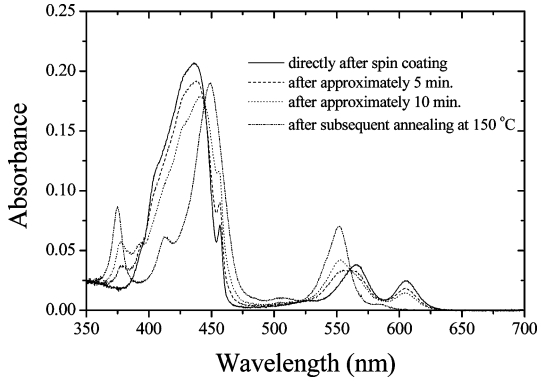

Figure 4. Absorption spectra of a ZnTOPP film spin-coated from pyridine vs time.

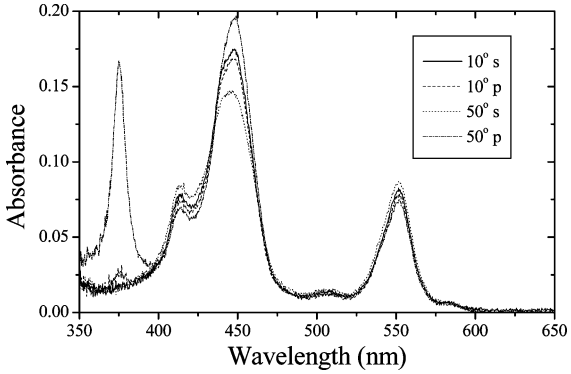

Figure 5. Polarized absorption spectra of ZnTOPP films spin-coated from 5 mM toluene solution onto quartz for two angles of incidence.

transition. The strong absorption bands at 425 (toluene) and 416 nm (hexane) with weak sidebands in the 350−490-nm region are assigned to the strongly allowed B transitions. By contrast, the absorption spectra of the ZnTOPP films show three or four different peaks, depending on the sample treatment. ZnTOPP spin-coated from toluene has absorption bands at 375, 413, and 450 nm, whereas ZnTOPP spin-coated from chloroform shows an additional band at 390 nm. This band disappears upon annealing of the film, however, as shown in Figure 3B. For ∼25-nm-thick films spin-coated from 5 mM toluene solution, the band at 450 nm seemed to consist of two components; however, spin-coated 5-nm-thick films from 1 mM solutions produced only a single band without shoulders, suggesting that the shoulder observed for the thicker film is due to reflection effects, which are expected to increase with the film thickness. ZnTPP films show only a single, broad, structureless absorption band centered at 440 nm. The 375 nm absorption band is also found in the fluorescence excitation spectra. Its intensity increases with increasing layer thickness, demonstrating that the observed polarization is a bulk property of the film and not that of a surface layer. This is further supported by the observation that in films spin-coated from pyridine this band is absent at first but fully reappears with time during slow evaporation of the solvent from the film (Figure 4).

The shifts and splittings of the B-bands in the films with respect to their position in dilute solutions may in principle result from (i) porphyrin−substrate interaction, (ii) the presence of different aggregates, (iii) excitonic interactions between neighboring porphyrin molecules in the film, or from combinations of i, ii, and iii. The interaction of type i should give rise to spectra that depend on the thickness of the film, which is not observed. Note also that the Q-band for the films is at almost the same wavelength as for solutions, supporting the conclusion that there are no strong porphyrin−substrate interactions. The two bands at 375 and 450 nm in the B-band region cannot be ascribed to the presence of two different types of aggregates either, since the results of fluorescence quenching measurements (paper 2) do not depend on the excitation wavelength. Efficient energy transfer between two different aggregates in the films as a possible cause of the occurrence of two bands can also be excluded, since the distance between aggregates is at least 5 times that between two porphyrin molecules within one stack, considering the presence of alkyl and phenyl substituents at each porphyrin macrocycle.

Therefore, the shift of the prominent ∼420-nm B-band in solution to 450 nm for the film and the splitting into three or four components must be ascribed to excitonic interactions, and possible effects of the change of the molecular environment can be neglected.

The B-bands of ZnTOPP films are similar to those of spin-coated films of H_2TOPP[27] and aggregates of ZnTPP derivatives in solution.[11−13] The B-band of these aggregates is split into a strong red-shifted component and a weak blue-shifted component. Similar splittings have been reported for porphyrin LB films.[28,29] For the aggregated derivative reported in refs 11−13 with a molecular structure closely resembling that of ZnTOPP, the B-band has two main components, i.e., at 446 and 375 nm, very similar to the 450 and 375 nm bands for the ZnTOPP films in this work. The 413 nm absorption band of ZnTOPP films was found to be absent for the aggregates in solution. This band is very close to the B-band of ZnTOPP in hexane (cf. Figure 2) and can be related either to ZnTOPP monomers embedded in the alkyl side chains of the ZnTOPP aggregates or to an excitonic shift of the B-band resulting from a slightly different geometry of the aggregates in the film as compared to that in solution.

Polarized Absorption Spectra. The strong polarization anisotropy of the absorption spectra at different incidence angles α, as shown in Figure 5, indicates that the ZnTOPP molecules in the film spin-coated from toluene are highly ordered. Defining the absorbance at perpendicular and parallel polarization as A_s and A_p, respectively, from the 375-nm absorption at different incidence angles α (Figure 5) the reduced linear dichroism

$$LD^r = \frac{A_p - A_s}{A_p + 2A_s} \quad (1)$$

is calculated to be 0.9 ± 0.05, demonstrating that this band results from a highly ordered molecular array with a polarized transition parallel to the plane of incidence, i.e., the transition dipole moment *M* associated with this band is perpendicular to the substrate. Since *M* is in the molecular plane, this implies that all porphyrin planes in the stacks are perpendicular to the substrate plane. In agreement with this, the intensity of the 375-nm band decreases with the decreasing incidence angle as shown in Figure 6 and completely disappears in spectra recorded at a normal incidence of the exciting light. The polarization of the 450-nm red-shifted band appears to be perpendicular to the substrate plane, but reflection effects at this wavelength are too strong to justify a conclusion about its polarization. At 375 and 450 nm, A_s and A_p at $\alpha = 10°$ are almost equal, indicating that the absorbance is averaged in the substrate plane over the angle φ (Figure 7A), i.e., there is no preferential orientation of the various domains around the normal to the substrate plane, resulting in averaging of the orientational distribution of the domains and thus of the stacks within the illuminated area. This implies that optical polarization data only yield information on the orientation of the porphyrin molecular plane with respect

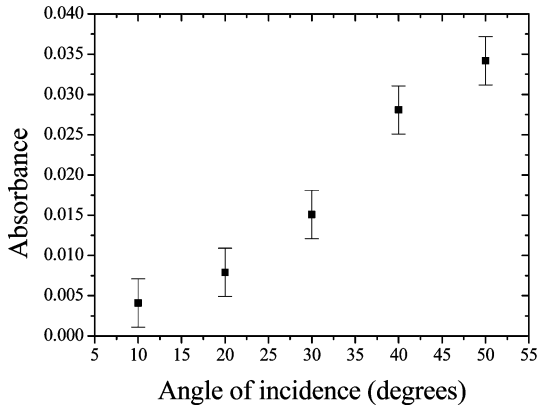

Figure 6. Absorbance at 375 nm of a spin-coated ZnTOPP film vs the angle of incidence.

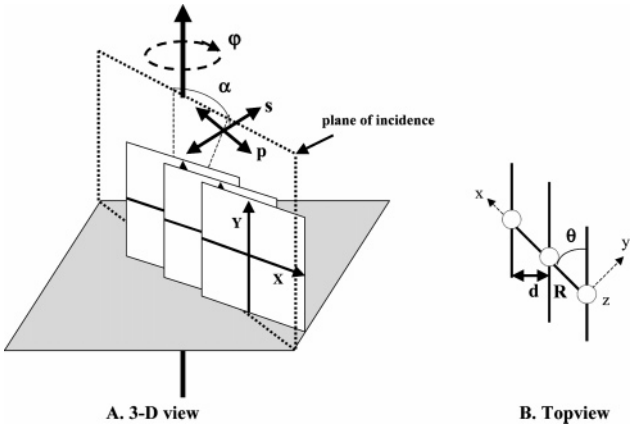

Figure 7. Structural arrangement of a slipped-deck-of-cards array. (A) In the three-dimensional view, the angle α is the incidence angle; rotation around φ takes the random orientation of the stacks in the substrate plane into account. (B) In the top view, θ is the angle between the line connecting the porphyrin centers and the porphyrin molecular planes. Note that the laboratory frame of reference $\{x,y,z\}$ of part B does not coincide with the molecular frame of reference $\{X,Y,Z\}$.

to the substrate and not on the mutual orientation of the porphyrin planes in the stack with respect to each other. To determine the mutual orientation and position of the porphyrin monomers in a stack, additional information is required, e.g., the number of exciton components, the most stable ground-state conformation of oligomers in solution, and/or the crystal structure.

The spectral effects of the excitonic interactions between the two degenerate transition moments of metalloporphyrins for various dimer geometries are well-known.[30] For a parallel porphyrin array and transitions from the ground state to the excited state, two exciton states are forbidden for one pair and allowed for another pair, with mutually perpendicular polarization. For a cofacial dimer, there are two allowed blue-shifted transitions at the same energy.

If the monomers are alternately shifted in two perpendicular directions, resulting in helical or zigzag-type aggregates, there is only one allowed transition to a twofold degenerate exciton state, giving rise to a red or blue spectral shift, depending on the angle θ between the molecular planes and the center-to-center vector. For translationally shifted parallel arrays denoted as "slipped-decks-of-cards", this degeneracy is lifted, one of the allowed transitions always being blue-shifted, whereas the other transition can be blue- or red-shifted from the monomer position, depending on the angle between the center-to-center vector and the molecular planes. Edge-to-edge or corner-to-

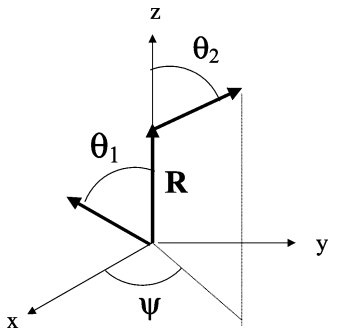

Figure 8. Axis system for the calculation of the dipole−dipole excitonic interaction.

corner shifted arrays (or any other shift direction as long as the dimer is parallel) yield identical results. The blue-shifted transition (or one of the two if there are two blue-shifted transitions) is always polarized perpendicular to the shift direction. For tetrasulfophenyl porphyrin aggregates in solution, absorption bands red- and blue-shifted with respect to the monomer B-band have indeed been found.[31] Flow-induced linear dichroism measurements have shown that the transition dipole moments of these bands are mutually perpendicular, where the red-shifted band was found to be polarized along the long axis of the aggregate and the blue-shifted band along the short axis, in agreement with the dipole−dipole exciton model for J-type linearly aggregated porphyrins.

For arrays containing mutually tilted molecular planes, in principle, transitions to each of the four exciton states are allowed.

A tilted configuration is highly unlikely, however, in view of the symmetry of the porphyrin monomers constituting the array. In fact, crystal structures of tetraphenyl porphyrins[32−34] and NMR spectra[35] of porphyrin dimers and oligomers in solution invariably show that adjacent porphyrins in dimers, at least in their ground state, preferably assume a slipped-deck-of-cards configuration. Such an arrangement is also supported by fluorescence anisotropy decay measurements (paper 2).

Spectral shifts and splittings for porphyrin aggregates have frequently been explained by the Kasha dipole−dipole exciton model[36,37] using a single transition dipole moment for each of the monomers in the aggregate. Similar to what occurs for aggregates with a single transition dipole moment per monomer, for large aggregates of ZnTOPP monomers with two degenerate transition dipole moments, both the number of exciton states and the exciton bandwidth increase. The number of allowed transitions and the direction of their spectral shifts compared to the monomer band remain the same, but the magnitude of the shift approaches twice the interaction potential V by increasing the aggregate size.

The dipolar interaction potential V is given by[36−38]

$$V_{ij} = V_{ji} = V_0[\sin\theta_1 \sin\theta_2 \cos\psi - 2\cos\theta_1 \cos\theta_2] \qquad i,j = X,Y \quad (2)$$

where the angles θ_1, θ_2, and ψ are defined in Figure 8 and

$$V_0(\text{eV}) = 6.24 \times 10^{-4}\frac{M^2}{\epsilon_r R^3} = 6.24 \times 10^{-4}\frac{M^2}{\epsilon_r d^3}\sin^3\theta \quad (3)$$

with M expressed in Debye units, R and d in nanometers, ϵ_r the high-frequency dielectric constant, and d the distance between the molecular planes.

Since we assume that the molecular planes in the aggregate are parallel, $\psi = 0$ and $d = R \sin\theta$ (Figure 7B). For parallel

and cofacial arrays, the off-diagonal elements $V_{XY} = V_{YX} = 0$, since in a common laboratory axis system the molecular *X*- and *Y*-transition moments of adjacent porphyrins in this array are perpendicular.

A linear array of a slipped-deck-of-cards is predicted to have two allowed exciton states with orthogonal transition dipole moments, resulting in blue- and red-shifted B-bands with mutual perpendicular polarization.

Recently, it has been shown[39] that intensity from the red-shifted exciton component can be transferred to the Q-band by nonzero values of $V_{XY} = V_{YX}$ or higher-order Coulombic perturbation terms in the Hamiltonian, resulting in enhanced intensity of this band, as is indeed experimentally found (Figure 2).

These observations are in agreement with the structure of the films containing linear porphyrin stacks with a slipped-deck-of-cards geometry, with their long axis parallel to the substrate. Then, the 375-nm band of the ZnTOPP stacks corresponds to a transition with a polarization along the short axis of the stacks. Since the 375-nm band has been found to be a bulk property of the film, we may conclude that the film has a lamellar structure.

The 450-nm band results from two contributions:

(i) interaction of the incident parallel and perpendicularly polarized light with the *X*-component of *M* averaged over the angle φ (Figure 7A), giving rise to absorbances $A_{p(av)}$ and $A_{s(av)}$

(ii) reflection effects, resulting in additional polarization with unknown magnitude and sign. Unfortunately, this contribution prevents an accurate prediction of the net polarization of the red-shifted exciton component.

According to the Kasha model, the transition energy of an aggregate (ΔE_{agg}) is given by[36,37]

$$\Delta E_{agg} = \Delta E_{mon} + \Delta D \pm 2V \tag{4}$$

where ΔE_{mon} is the transition energy of the monomer, ΔD is the difference between the van der Waals terms for the ground and the excited state, assumed to be equal for the ground and excited state, and $2V$ is the exciton interaction energy for an aggregate of *N* monomers, with *N* a large number, as is assumed to apply to the porphyrin stacks.

For $\theta_1 = \theta_2 = \theta$ and $\psi = 0$, eq 2 transforms to

$$V_{ij} = V_{ji} = V_0(1 - 3\cos^2\theta) \quad i,j = X,Y \tag{5}$$

with θ the angle between the center-to-center vector *R* and both transition dipole moments[36,37] (Figure 7B). Since *M* lies in the porphyrin plane, θ is also the angle between the center-to-center vector and that plane. The energy of the blue-shifted transition is given by substituting $\theta_1 = \theta_2 = 90°$ in eq 5, yielding $\epsilon^{blue} = 2V_{YY} = 2V_0$. However, $\epsilon^{red} = 2V_{XX} = 2V_0(1 - 3\cos^2\theta)$. Thus, θ can be calculated from

$$\epsilon^{red}/\epsilon^{blue} = (1 - 3\cos^2\theta) \tag{6}$$

Through the use of the B-band of the porphyrin in hexane at $\lambda_0 = 416$ nm as a reference, the shifts of the 375 and 450 nm exciton bands are calculated as 0.326 and 0.225 eV, respectively, resulting in $\theta \approx 41°$. If we use the absorption band of the porphyrin in toluene at $\lambda_0 = 425$ nm, then θ changes to $\sim 47°$. It is interesting to note that these angles are close to that in the ground state of dimers of zinc tetraphenylporphyrin derivatives in solution. NMR ring current shifts for these solution dimers yield a parallel conformation with a 0.42-nm translation along the phenyl−phenyl axis and a plane-to-plane distance of 0.31 nm,[35] resulting in $\theta \approx 40°$. Considering the striking agreement between the value of θ for the film and in solution, we may draw a cautious conclusion that the internal relative dielectric constant of the film is rather low and equals $\epsilon_r \approx 2-3$. Substituting $\epsilon_r = 1.89$ for hexane, $M = 9.5$ D for the B-band, calculated from the solution spectra, the previously determined angle $\theta = 41°$, and the blue shift of 0.326 eV into eq 3, the distance *d* between two adjacent porphyrins is calculated to be 0.37 nm. Replacing these data by those for toluene ($\epsilon_r \approx 2.24$, $\lambda_0 = 425$ nm) as a reference results in $\theta = 47°$ and $d = 0.36$ nm and thus does not lead to significant changes in the interplanar distance. For both media, the calculated value of *d* is again rather close to the ground-state value of 0.31 nm, supporting our previous conclusion that most likely the internal dielectric constant of the film is $\sim 2-3$.

For the S_2 exciton to be observable in the absorption spectrum, the excitonic interaction energy in frequency units must exceed the lifetime broadening of the S_2 excited state, which is $(2\pi\tau)^{-1}$ with τ its lifetime. For a substituted zinc porphyrin monomer similar to ZnTOPP, $\tau \approx 1-2$ ps, resulting in $\tau^{-1}(S_2) \approx (0.5-1) \times 10^{12}$ s^{-1}. For its linked porphyrin arrays, τ has been found to be <1 ps[40], however, and the same shortening of τ may be expected for the S_2 lifetime in the porphyrin arrays in this work. The fact that both excitonic components, i.e., the blue- as well as the red-shifted one, are observed implies that the lifetime broadening of the S_2 excited state must be considerably less than the excitonic interaction energy of $\sim 1.3 \times 10^{14}$ s^{-1} derived from the splitting between the 375 and 450 nm excitonic bands.

As predicted by the dipole−dipole exciton model, the Q-bands do not show any splitting or shift, due to their much smaller transition moments $M \approx 0.7$ D for Q(0,0), and remain twofold degenerate**.** Even though the porphyrins are oriented perpendicularly to the substrate, the Q-bands do not exhibit any polarization. As stated before, the Q-bands will predominantly mix with the red-shifted exciton component of the B-band as compared with the blue-shifted component,[39] resulting in an increase of the transition moment of the Q-band parallel to the substrate. This effect, together with the random orientation of this transition moment, explains the vanishing of the Q-band polarization. The absorbances resulting from the interaction of the electric component *E* of the incident light with each of the two perpendicular transition moments add up. Averaging over all orientations of the stacks in the substrate plane and assuming that the components E_s and E_p are equal results in the disappearance of the Q-band polarization.

At the calculated interplanar distance of less than 0.4 nm between adjacent porphyrins, a simple point dipole model is at the limit of its validity and may even break down. The point dipole approximation is only valid when the distance between the molecules is roughly larger than their size,[41] which does not apply to the above-mentioned type of aggregates. Using an extended dipole model[42,43] does not change the essence of the discussion above, however, since it has been found to lead to only minor corrections for *d* and θ.

A film structure with a linear slipped-deck-of-cards arrangement is similar to that proposed for porphyrin LB films[28,29] and aggregates in solution.[12] Atomic force microscopy of supramolecular porphyrin monolayers deposited from solution on graphite has shown that the monomers in these layers are cofacial and perpendicularly oriented on the substrate[10] as in the present work.

Recently, Monte Carlo simulations have been applied to the same ZnTOPP films using preliminary results from the present work on the film structure and comparing the simulated data

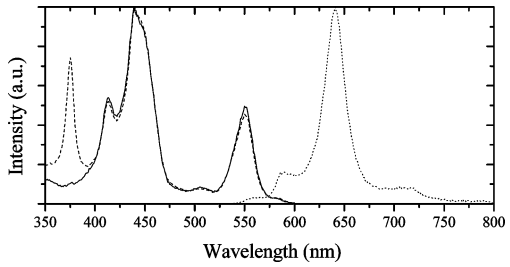

Figure 9. Emission and excitation spectra: solid line, excitation spectrum at normal incidence, $\lambda_{em} = 640$ nm; dashed line, excitation spectrum at 45° angle of incidence, $\lambda_{em} = 640$ nm; dotted line, emission spectrum, $\lambda_{exc} = 450$ nm.

with the experimental energy-transfer kinetics.[44] The results of these simulations have shown that the above-mentioned structural model of the nanolayers is essentially correct.

Annealing Effects. Figure 3 illustrates the changes in the room-temperature absorption spectra of ZnTOPP films following annealing to 175 °C during ~5 min, resulting in the formation of ordered domains.[11−13] For ZnTOPP films **1**, annealing leaves the shape and width of the B-band unaffected. By contrast, the 390-nm band for films **2** disappears upon annealing, and the full width at half-maximum (fwhm) line width of the B-band at 450 nm decreases from 27 ± 1 nm (1400 cm^{-1}) to 24 ± 1 nm (1200 cm^{-1}). After annealing, the spectrum of film **2** is identical to that of **1.** By contrast, Figure 3C shows that annealing of ZnTPP films spin-coated from toluene or chloroform results in considerable broadening of the B-band, i.e., from 35 ± 3 nm (1800 cm^{-1}) to 59 ± 3 nm (3000 cm^{-1}). Also, whereas the 450 nm B-band of the ZnTOPP film is red-shifted by ~25 nm from that in solution spectra, the B-band of ZnTPP is on average only ~10 nm red-shifted. For the ZnTOPP films, the Q-bands around 550 nm are unaffected by annealing, but the Q-bands of ZnTPP films **3** show a small blue shift and a small change in the intensity ratio $I_{Q(0,0)}/I_{Q(1,0)}$ (Figure 3C). These changes are similar to those observed upon drying a solution of ZnTPP in toluene on sodium wire, and we therefore ascribe these changes to the removal of an aquo ligand. We suggest that the broadening upon annealing is due to the decrease in the intermolecular distance between the porphyrin molecules in the film by removal of the aquo ligands, thereby increasing the intermolecular excitonic interaction. However, from the intensity ratio and positions of the Q-bands of ZnTOPP films spin-coated from nondried toluene, we conclude that ZnTOPP in these films is not bound to an aquo ligand. This is also supported by the finding that sodium-drying of toluene before use and storing the film for several weeks in the dark and ambient air leaves the spectra unchanged. These results strongly indicate that the octyl chains in ZnTOPP screen the porphyrin core of the aggregates from atmospheric moisture.

The molecular ordering inside the films is reflected by their absorption and fluorescence spectra (Figures 3 and 9). Whereas in films **1** the 450-nm B-band has about the same width before and after annealing (Figure 3A), the narrowing of this band in films **2** (Figure 3B) upon annealing indicates a transition to a more ordered film structure[45−47]

The 390-nm band in the absorption spectra of films **2** spin-coated from chloroform is absent in spectra of ZnTOPP in the same solvent, implying that this band is a property of the film. From the low-temperature fluorescence spectra, we may conclude that after exposure to chloroform a large fraction of the ZnTOPP molecules has been changed to the ligated form, acting as fluorescent traps.[48] (For details, see paper 2.)

The most likely explanation for the effect of exposure of the film to chloroform in liquid or gaseous form is that it disrupts the interaction between the porphyrin octylchains and thus the molecular ordering of the stacks. The equivalence of the porphyrins within a stack is thereby destroyed, and as a result the excitonic interaction is reduced or even disappears, depending on the remaining degree of order. Similar to what happens in ZnTPP films, the ZnTOPP molecules are now exposed to traces of water, which are always present in the solvent. Water may act as a weak aquo ligand to the porphyrin zinc center, resulting in the formation of excitation traps within each stack. We cannot completely exclude that chloroform itself could be the ligand instead of water, but this is less likely, since chloroform is not known to have ligating properties. Whatever the ligand is, upon annealing of the film, chloroform evaporates from the film, and its order as well as the excitonic interactions between the ZnTOPP molecules are restored; i.e., the 390-nm band shifts back to 375 nm, and the 450-nm band shifts slightly to the red as shown in Figure 3. To investigate this phenomenon further, we also prepared films by spin-coating from the strongly ligating pyridine as a solvent. Figure 4 shows the room-temperature absorption spectra of ZnTOPP films spin-coated from pyridine (film **4**). Immediately after spin-coating (Figure 8), the (0,0) and (0,1) Q-bands are red-shifted compared to those of the films spin-coated from chloroform (**2**) or toluene (**1**), with a concomitant increase of the intensity ratio $I_{Q(0,0)}/I_{Q(0,1)}$. These features identify the species as pyridine-ligated ZnTOPP[48−50] The B-band is split into several components, with the main component at 437 nm broadened with respect to the same band in films **1**. Note that in this spectrum the 375-nm absorption band is absent. Slow evaporation of pyridine from the film results in a gradual blue shift of the Q-bands and a return of the $I_{Q(0,0)}/I_{Q(0,1)}$ intensity ratio to that of film **1**. Furthermore, we note that the B-bands initially have shoulders at 390 and 400 nm. The 390-nm band gradually disappears during evaporation of the solvent in favor of the 375-nm polarized absorption band, and the entire B-band narrows and shifts to 450 nm. Only after annealing at 150 °C, the film becomes completely ordered (Figure 4). Exposing film **1** to pyridine vapor results in essentially the same spectral changes. The origin of the 390-nm band is somewhat unclear. Note that it appears in both spectra of films spin-coated from chloroform as well as from pyridine, even though these solvents have quite different ligand strengths. This could be an indication that it arises from a modified excitonic interaction between less ordered porphyrins, as a result of their interaction with the solvent.

Since the above-mentioned experiments lead to complete conversion of the nonligated to the ligated ZnTOPP species, we may again conclude that the 375-nm absorption band is a bulk property of the film.

There is an important difference between the spectral effects of exposure of the film to chloroform and pyridine vapor. Treatment of ZnTOPP films with chloroform vapor does not result in a net shift of the B-band as occurs with pyridine. Obviously, the effect of chloroform represents a more subtle change of the porphyrin environment in the ordered film, in particular of the excitonic interaction with neighboring porphyrins, than with pyridine. These changes only occur at low temperature since room-temperature absorption spectra of ZnTOPP in neat chloroform and toluene are identical. Evidently, chloroform interacts only weakly with ZnTOPP molecules in the film, reducing the excitonic interaction, but without completely destroying its order, as occurs with pyridine as a ligand.

The changes in the film structure as revealed by the absorption spectra can be summarized as follows:

- Films **1** show spontaneous ordering.
- Chloroform has a disordering effect on the films, as demonstrated for films **2** and **3**, most likely by exposing the porphyrins to traces of water, acting as aquo ligands to the porphyrin zinc centers.
- Interaction with strong ligands, e.g., pyridine, as in film **4**, disrupts the molecular ordering of the films, which is restored upon evaporation of the solvent.

Acknowledgment. T.J.S. thanks Dr. Herbert van Amerongen for useful comments. This work was supported by The Netherlands Organization for Energy and Environment under Contract No. 146.100-024.4.

References and Notes

(1) *Springer Handbook of Nanotechnology*; Bushan, B., Ed.; Springer-Verlag: New York, 2004.
(2) Ohring, M. *The Materials Science of Thin Films*; Elsevier Science and Technology Books: Amsterdam, The Netherlands, 2001.
(3) Tredgold, R. H. *Order in Organic Films*; Cambridge University Press: New York, 1994.
(4) Frank, C. W. *Organic Thin Films: Structure and Applications*; ACS Symposium Series 695; American Chemical Society: Washington, DC, 1998.
(5) Wöhrle, D.; Meissner, D. *Adv. Mater.* **1991**, *3*, 129.
(6) Liu, C.-Y.; Bard, A. J. *Acc. Chem. Res.* **1999**, *32*, 235.
(7) Peumans, P.; Yakimov, A.; Forrest, S. R. *J. Appl. Phys.* **2003**, *93*, 3693.
(8) Drain, C. M.; Hupp, J. T.; Suslick, K. S.; Wasielewski, M. R. *J. Porphyrins Phthalocyanines* **2002**, *6*, 243.
(9) Friedrich, M.; Gavrila, G.; Himcinschi, C.; Kampen, T. U.; Kobitski, A. Yu.; Méndez, H.; Salvan, G.; Cerrilló, I.; Méndez, J.; Nicoara, N.; Baró, A. M.; Zahn, D. R. T. *J. Phys.: Condens. Matter* **2003**, *15*, 2699.
(10) Guo, Q.; Yin, J.; Yin, F.; Palmer, R. E.; Bampos, N.; Sanders, J. K. M. *J. Phys.: Condens. Matter* **2003**, *15*, 3127.
(11) Kroon, J. M.; Sudhölter, E. J. R.; Schenning, A. P. H. J.; Nolte, R. J. M. *Langmuir* **1995**, *11*, 214.
(12) Kroon, J. M.; Schenkels, P. S.; van Dijk, M.; Sudhölter, E. J. R. *J. Mater. Chem.* **1995**, *5*, 1309.
(13) Kroon, J. M.; Koehorst, R. B. M.; van Dijk, M.; Sanders, G. M.; Sudhölter, E. J. R. *J. Mater. Chem.* **1997**, *7*, 615.
(14) (a) Koti, A. S. R.; Periasamy, N. *J. Mater. Chem.* **2002**, *12*, 2313. (b) Koti, A. S. R.; Periasamy, N. *Chem. Mater.* **2003**, *15*, 369.
(15) Shimizu, Y.; Miya, M.; Nagata, A.; Ohta, K.; Yamamoto, I.; Kusabayashi, S. *Liq. Cryst.* **1993**, *14*, 795.
(16) Shimizu, Y.; Higashiyama, T.; Fuchita, T. *Thin Solid Films* **1998**, *331*, 279.
(17) Chandrasekhar, S. In *Handbook of Liquid Crystals, Low Molecular Weight Liquid Crystals II*; Demus, D., Goodby, J., Gray, G. W., Spiess, H.-W., Vill, V., Eds.; Wiley-VCH: Weinheim, Germany, 1998; Vol. 2B, Chapter 8.
(18) *The Porphyrin Handbook*; Kadish, K. M., Smith, K. M., Guilard, R., Eds.; Academic Press: San Diego, Tokyo, 1999; Vols. 6 and 8.
(19) Ogi, T.; Ohkita, H.; Shinzaburo, I.; Masahide, Y. *Thin Solid Films* **2002**, *415*, 228.
(20) Hayashi, K.; Kawato, S.; Fujii, Y.; Horiuchi, T.; Matsushige, K. *Appl. Phys. Lett.* **1997**, *70*, 1384.
(21) Yokoyama, T.; Yokoyama, S.; Kamikado, T.; Mashiko, S. *J. Chem. Phys.* **2001**, *115*, 3814.
(22) Wienke, J.; Kleima, F. J.; Koehorst, R. B. M.; Schaafsma, T. J. *Thin Solid Films* **1996**, *279*, 87.
(23) Gouterman, M. In *The Porphyrins*; Dolphin, D., Ed.; Academic Press: New York, 1978; Vol. III, Chapter 1.
(24) Adler, A. D.; Longo, F. R.; Kampas, F.; Kim, J. *J. Inorg. Nucl. Chem.* **1970**, *32*, 2443.
(25) Adler, A. D.; Longo, F. R.; Shergalis, W. *J. Am. Chem. Soc.* **1964**, *86*, 3145.
(26) Little, R. G.; Anton, J. A.; Loach, P. A.; Ibers, J. A. *J. Heterocycl. Chem.* **1975**, *12*, 343.
(27) Kroon, J. M.; Sudhölter, E. J. R.; Wienke, J.; Koehorst, R. B. M.; Savenije, T. J.; Schaafsma, T. J. In *Proceedings of the 13th European Photovoltaic Solar Energy Conference*, Nice, France, Oct 1995; H. S. Stephens & Associates: Bedford, U.K., 1995; pp 1295−1298.
(28) Schick, G. A.; Schreiman, I. C.; Wagner, R. W.; Lindsey, J. S.; Bocian, D. F. *J. Am. Chem. Soc.* **1989**, *111*, 1344.
(29) Azumi, R.; Matsumoto, M.; Kawabata, Y.; Kuroda, S.; Sugi, M.; King, L. G.; Crossley, M. J. *J. Phys. Chem.* **1993**, *97*, 12862.
(30) Tran-Thi, T. H.; Lipskier, J. F.; Maillard, P.; Momenteau, M.; Lopez-Castillo, J. L.; Jay-Gerin, J.-P. *J. Phys. Chem.* **1992**, *96*, 1073.
(31) Ohno, O.; Kaizu, Y.; Kobayashi, H. *J. Chem. Phys.* **1993**, *99*, 4128.
(32) Hamor, M. J.; Hamor, T. A.; Hoard, J. L. *J. Am. Chem. Soc.* **1964**, *86*, 1938.
(33) Fleischer, E. B.; Miller, C. K.; Webb, L. E. *J. Am. Chem. Soc.* **1964**, *86*, 2342.
(34) Silvers, S. J.; Tulinsky, A. *J. Am. Chem. Soc.* **1967**, *89*, 3331.
(35) Hofstra, U.; Koehorst, R. B. M.; Schaafsma, T. J. *Magn. Reson. Chem.* **1987**, *25*, 1069.
(36) McRae, E. G.; Kasha, M. *J. Chem. Phys.* **1958**, *28*, 721.
(37) Kasha, M.; Rawls, H. R.; El-Bayoumi, M. A. *Pure Appl. Chem.* **1965**, *11*, 371.
(38) Stomphorst, R. G.; Schaafsma, T. J.; van der Zwan, G. *J. Phys. Chem. A* **2001**, *105*, 4226.
(39) Zimmermann, J.; Siggel, U.; Fuhrhop, J.-H.; Röder, B. *J. Phys. Chem. B* **2003**, *107*, 6019.
(40) Cho, H. S.; Song, N. W.; Kim, Y. H.; Jeoung, S. C.; Hahn, S.; Kim, D. *J. Phys. Chem. A* **2000**, *104*, 3287.
(41) Förster, Th. *Ann. Phys.* **1948**, *2*, 55.
(42) Czikklely, V.; Forsterling, H. D.; Kuhn, H. *Chem. Phys. Lett.* **1970**, *6*, 207.
(43) Von Maltzan, B. *Z. Naturforsch., A: Phys. Sci.* **1985**, *40*, 389.
(44) (a) Yatskou, M. M., Ph.D. Thesis, Wageningen University, 2001. (b) Yatskou, M. M.; Donker, H.; Novikov, E. G.; Koehorst, R. B. M.; van Hoek, A.; Apanasovich, V. V.; Schaafsma, T. J. *J. Phys. Chem. A* **2001**, *105*, 9498. (c) Yatskou, M. M.; Donker, H.; Koehorst, R. B. M.; van Hoek, A.; Schaafsma, T. J. *Chem. Phys. Lett.* **2001**, *345*, 141. (d) Apanasovich, V. V.; Novikov, E. G.; Yatskou, M. M.; Koehorst, R. B. M.; Schaafsma, T. J.; van Hoek, A. *J. Appl. Spectrosc.* **1999**, *66*, 613.
(45) Gregg, B. A.; Fox, M. A.; Bard, A. J. *J. Phys. Chem.* **1989**, *93*, 4227.
(46) Markovitsi, D.; Lécuyer, I.; Simon, J. *J. Phys. Chem.* **1991**, *95*, 3620.
(47) Sigal, H.; Markovitsi, D.; Gallos, L. K.; Argyrakis, P. *J. Phys. Chem.* **1996**, *100*, 10999.
(48) Humphrey-Baker, R.; Kalyanasundaram, K. *J. Photochem.* **1985**, *31*, 105.
(49) Nardo, J. V.; Dawson, J. H. *Inorg. Chim. Acta* **1986**, *123*, 9.
(50) Miller, J. R.; Dorough, G. D. *J. Am. Chem. Soc.* **1952**, *74*, 3977.